Metal-semiconductor transition and Luttinger-liquid behavior in quasi-one-dimensional $BaVS_3$ studied by photoemission spectroscopy

M. Nakamura,* A. Sekiyama, H. Namatame,† and A. Fujimori
Department of Physics, University of Tokyo, Bunkyo-ku, Tokyo 113, Japan

H. Yoshihara and T. Ohtani
Laboratory for Solid State Chemistry, Okayama University of Science, Ridai-cho 1-1, Okayama 700, Japan

A. Misu
Department of Physics, Science University of Tokyo, Shinjuku-ku, Tokyo 116, Japan

M. Takano
Institute for Chemical Research, Kyoto University, Uji, Kyoto 611, Japan
(Received 23 December 1993)

The quasi-one-dimensional conductor $BaVS_3$ exhibits successive phase transitions at ~ 240 K (linear chains to zigzag chains), ~ 70 K (metallic to semiconducting), and ~ 35 K (paramagnetic to antiferromagnetic). We have made high-resolution ultraviolet-photoemission-spectroscopy (UPS), x-ray-photoemission-spectroscopy, electrical-resistivity, and magnetic-susceptibility measurements on $BaVS_3$. UPS spectra near the Fermi level of the metallic phase exhibit a power-law dependence on the electron binding energy, indicating that conduction electrons in $BaVS_3$ behave as a Luttinger liquid. The power-law exponent is large ($< \sim 1$), indicating that electron-electron interaction is long ranged and possibly that electron-phonon interaction is also important. The spectra exhibit gradual changes with temperature. In particular, a semiconducting gap starts to open well above the metal-to-semiconductor transition temperature and fully develops below it. We propose that the gradual orthorhombic distortion of the Jahn-Teller type below ~ 240 K lowers one of the d levels, d_{xy}, and that below ~ 70 K electrons are fully transferred to the d_{xy} band. The d_{xy} band then becomes half-filled, resulting in the opening of a Mott-Hubbard gap.

I. INTRODUCTION

Recently, there has been increasing interest in the unusual physical properties of correlated one-dimensional electron systems. According to Peierls,[1] an atomic chain with a partially filled conduction band lowers its energy by undergoing a periodic lattice distortion, which opens a gap at the Fermi level. If there is finite interaction between electrons, the Fermi-liquid state of a one-dimensional metal becomes unstable and the system becomes a Luttinger liquid.[2–4] The momentum distribution function of the Luttinger liquid shows a power-law singularity at the Fermi momentum. Recent theoretical studies based on g-ology analysis,[5] Monte Carlo simulations,[6] and conformal field theory[7–9] have yielded considerable insight into one-dimensional electron systems. Power-law exponents in the spin- and charge-correlation functions determine a number of physical properties on a low-energy scale.[10] As there exist rigorous relations between those exponents and the singularity exponent in the momentum distribution function,[8,10] experimental information about one of these numbers enables us to reveal the nature of the one-dimensional electron systems.

Photoemission spectroscopy is a useful tool to investigate the correlation exponents since it directly probes the single-particle spectral function, which shows a power-law dependence on the electron binding energy near the Fermi level, with the exponent identical to that in the momentum distribution function.[11] Recently, Dardel and co-workers[12,13] and Hwu *et al.*[14] studied quasi-one-dimensional metals such as $(TMTSF)_2PF_6$, $K_{0.3}MoO_3$, and $(TaSe_4)_2I$ using high-resolution photoemission spectroscopy. They found that the photoemission intensity at the Fermi level of these compounds is suppressed, and they attributed the observation to the characteristic behavior of Luttinger liquids.

In the present paper, we have studied the quasi-one-dimensional compound $BaVS_3$, which exhibits a number of intriguing physical properties. It has a crystal structure of the $BiNiO_3$ type,[15–17] as shown in Fig. 1, where face-sharing VS_6 octahedra form linear chains running along the c axis. The V-V distance within the chain is 2.84 Å, which is much shorter than the interchain V-V distance of 6.72 Å. It shows "metallic" conductivity and Curie-Weiss-like behavior of the magnetic susceptibility above ~ 70 K. Three phase transitions have been identified at ~ 240, ~ 70, and ~ 35 K. A crystal distortion occurs at ~ 240 K from the hexagonal structure to an orthorhombic structure[18–22] in which the linear V chains turn into zigzag chains.[19] (Note that the size of the unit cell is not doubled by the zigzag-chain formation.) Below ~ 70 K, the electrical resistivity steeply increases,[17,22] indicating a metal-to-semiconductor transition, accompanied by a sharp peak in the magnetic sus-

 ©1994 The American Physical Society

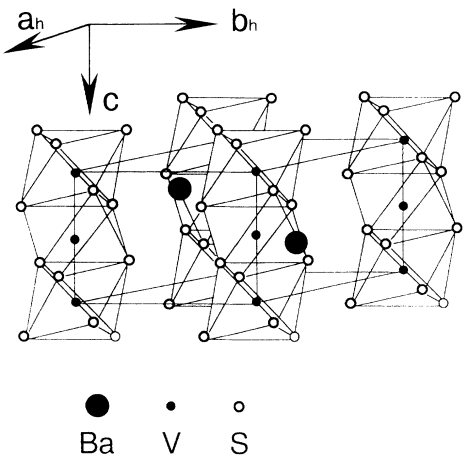

FIG. 1. Crystal structure of $BaVS_3$. The figure shows the structure of the hexagonal phase, where linear V chains are running along the c axis. Below ~ 240 K, the linear chains become zigzag ones. Here a_h and b_h stand for the hexagonal a and b axes (Ref. 15).

ceptibility[17] and an abrupt increase in the orthorhombic distortion within the ab plane without a change in the crystal symmetry.[19] Although the peak in the magnetic susceptibility at ~ 70 K is suggestive of an antiferromagnetic transition, no magnetic ordering has been found in neutron-diffraction[23] and NMR experiments.[24] Instead, the transition has been explained as due to the onset of a gradual pairing of magnetic V ions,[24] or that of a gradual electron transfer from localized magnetic states to nonmagnetic band states,[25] but no conclusive picture has emerged so far. At ~ 35 K, the susceptibility shows a minimum, and the slope of the electrical resistivity decreases below this temperature.[17] High-resolution inelastic neutron spin-flip scattering[26] and the NMR experiments[24] confirmed the ~ 35-K transition to be of the antiferromagnetic origin. As for the spectroscopic information on the electronic structure, Itti *et al.*[27] have reported x-ray and ultraviolet photoemission spectra of $BaVS_3$ and $BaV_{1-x}Ti_xS_3$, and found that the V $3d$ band is located close to the Fermi level, in general agreement with the results of a recent band-structure calculation.[28]

In the present study, we have focused on the high-resolution ultraviolet photoemission spectra near the Fermi level, and their changes across the metal-to-semiconductor transition. Core-level x-ray-photoemission spectra, magnetic susceptibility, and electrical resistivity have also been measured and utilized to characterize the nature of the phase transition. As a driving mechanism of the metal-insulator transition at ~ 70 K, we propose a model in which the V $3d$ band is split into subbands due to the orthorhombic lattice distortion of the cooperative Jahn-Teller type. Based on the correlation exponents deduced from the photoemission spectra, we discuss the inherent instability of the Luttinger liquid leading to the observed metal-to-semiconductor transition.

II. EXPERIMENT

Polycrystalline pellets of $BaVS_3$ were prepared as follows. A stoichiometric mixture of elemental Ba, V, and S was sealed in an evacuated silica tube and heated for two days at 800 °C. The starting materials were treated in a dry box filled with purified nitrogen. To avoid the reaction of Ba metal with the silica tube, the inside of the tube was coated with thin carbon film made by firing acetone. Obtained specimens were ground thoroughly and pelletized under a 2000 kg/cm^2 pressure, sintered for three days in the silica tube at 600 °C, and then slowly cooled to room temperature. The samples were checked to be single phase by x-ray diffraction.

Electrical resistivity was measured by employing a standard four-probe technique. Thermoelectric power from 90 to 273 K was measured under the temperature gradient of ~ 3 K/cm. Magnetic susceptibility was measured using a Quantum Design superconducting quantum interference device (SQUID) magnetometer. The applied magnetic field was 10 kOe.

Photoemission experiments were performed using a spectrometer equipped with a Mg/Al twin anode x-ray source (Mg $K\alpha$:$h\nu = 1253.6$ eV; Al $K\alpha$:$h\nu = 1486.6$ eV) for x-ray-photoemission spectroscopy (XPS), and a He discharge lamp (He I: $h\nu = 21.21$ eV; He II: $h\nu = 40.8$ eV) for ultraviolet photoemission spectroscopy (UPS). Photoelectrons were collected using a Vacuum Science Workshop hemispherical analyzer with a 150-mm radius. The analyzer chamber is magnetically shielded with μ metal. The base pressure of the analyzer chamber was $\sim 1\times 10^{-10}$ Torr, and the operating pressure of UPS was 1.8×10^{-9} Torr. The samples were cooled using a closed-cycle He refrigerator. The sample temperature was varied from 20 to 400 K using a ceramic heater. The temperature was monitored using a gold-0.07% iron-chromel thermocouple attached to the copper sample holder. Errors in the measured temperature were estimated to be -0 to $+5$ K. The best total resolution was evaluated to be ~ 22 meV by fitting the Au Fermi edge using a nearly flat density of states multiplied by the Fermi-Dirac distribution function and broadened with a Gauss function using the least-squares fitting method (see the inset of Fig. 6). The calibration of binding energies was achieved by measuring the Fermi edge of Au evaporated onto the sample. The energy resolution was ~ 1 eV for XPS and ~ 22 or ~ 60 meV for UPS depending on the analyzer pass energy used. In order to obtain clean surfaces, the samples were scraped *in situ* with a diamond file. We continually monitored the O $2p$, O KLL Auger, and C $1s$ signals to check for contamination on the sample surface.

III. RESULTS

A. Electrical resistivity and magnetic susceptibility

The temperature dependence of the electrical resistivity of one of the present samples is shown in Fig. 2. Above ~ 120 K the resistivity is low and nearly temperature independent, and below this temperature slightly increases down to ~ 75 K. It then sharply increases from ~ 70 to ~ 35 K, more slowly from ~ 35 to ~ 10 K, and again increases sharply below ~ 10 K. The result is in reasonable agreement with that reported by Takano

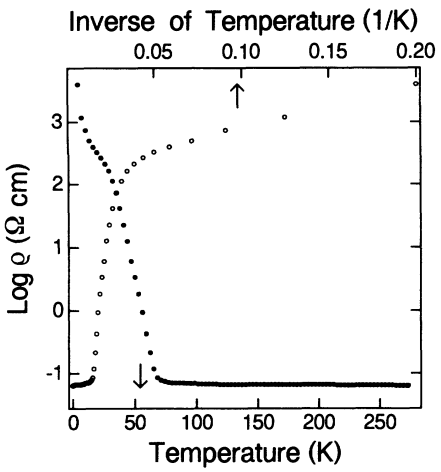

FIG. 2. Electrical resistivity ($\log_{10}\rho$) of $BaVS_3$, as a function of temperature. Changes in the slope are seen at ~70, ~35, and ~10 K.

et al.[17] The temperature-dependent activation energy E_a defined as

$$\rho(T) \propto \frac{E_a(T)}{k_B T} \tag{1}$$

is ~25 meV between ~70 and ~35 K. The thermoelectric power is negative for $T \gtrsim 100$ K, and is positive for $T \lesssim 100$ K as reported previously.[29]

The temperature dependence of the magnetic susceptibility χ is shown in Fig. 3(a). Between ~300 and ~80 K, it apparently obeys a Curie-Weiss law. A sharp peak and a dip appear at ~70 and ~40 K, respectively, consistent with the results of Takano *et al.*[17] In order to highlight anomalies in χ, we have plotted $d\chi/dT \times T^2$ as a function of T in Fig. 3(b). There one can see pronounced jumps at ~160 and ~70 K. Therefore, the susceptibility was fitted to a modified Curie-Weiss law:

$$\chi(T) = \chi_0 + \frac{C}{T-\Theta}\ , \tag{2}$$

where χ_0, C, and Θ represent a temperature-independent term, a Curie constant, and a Weiss constant, respectively, in each of the three temperature regions $T < 35$ K, 80 K $< T <$ 160 K, and $T > 160$ K, and the results are given in Table I. The Curie constant and hence the effective moment was found to be larger at $T > 160$ K ($1.11\mu_B$/mole) than at $T < 160$ K ($1.02\mu_B$/mole). These values are small compared with the spin-only value $2\sqrt{[S(S+1)]} = 1.73\mu_B$ for $S = \frac{1}{2}$ ($3d^1$) and the free-atomic value $g_J\sqrt{[J(J+1)]} = 1.55\mu_B$ for $J = \frac{3}{2}$. A close

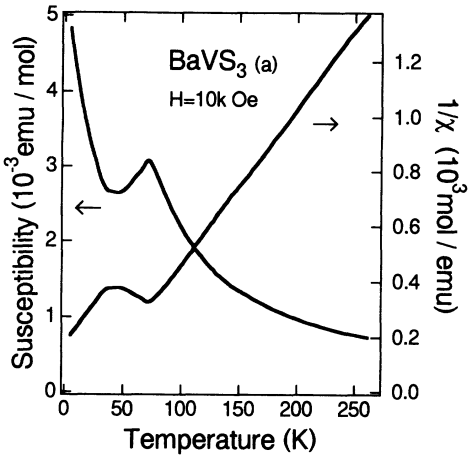

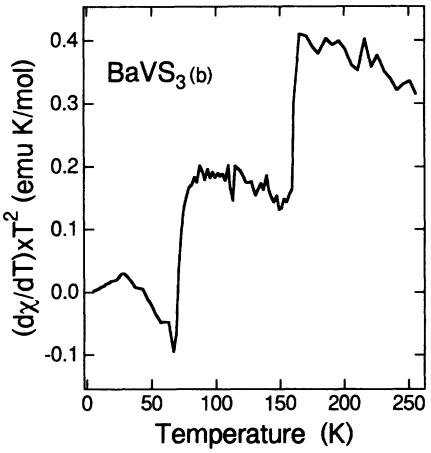

FIG. 3. (a) Magnetic susceptibility as a function of temperature. (b) Temperature derivative of the magnetic susceptibility, $T^2 d\chi/dT$. Anomalies are seen at ~160 and ~70 K.

examination of Fig. 3(b) reveals that the susceptibility already starts to be suppressed at ~90 K, well above the susceptibility peak at ~70 K. The absolute values of the effective moment and its change around $T \sim 160$ K generally agree with those reported by Kelber *et al.*[23]

B. Core levels

Figure 4 shows the S $2p$ and $2s$ and Ba $3d_{5/2}$ core-level spectra of $BaVS_3$. In going from ~300 to ~20 K, the S $2p$ and $2s$ peaks are shifted toward higher binding energies by ~0.1 eV, and the Ba $3d$ peaks by ~0.04 eV; other differences could not be detected within the accuracy

TABLE I. Least-squares fits of the magnetic susceptibility to a modified Curie-Weiss law $\chi = \chi_0 + C/(T-\Theta)$.

Temperature region	C (emu K/mole)	Θ (K)	χ_0 (emu/mole)	Effective moment (μ_B/mole)
300–160 K	0.131±0.002	45	1.24×10^{-4}	1.02
160–80 K	0.155±0.002	24	1.23×10^{-4}	1.11
<35 K	0.168±0.002	−30.5	1.24×10^{-4}	1.15

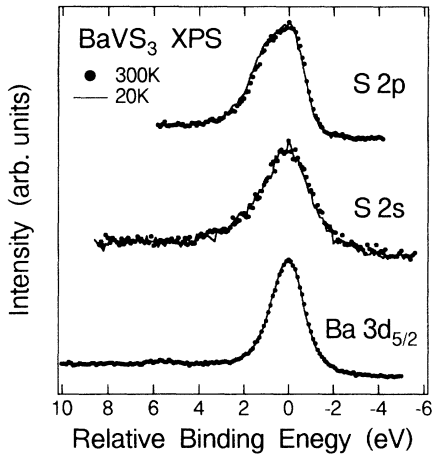

FIG. 4. S 2*p*, S 2*s*, and Ba $3d_{5/2}$ core-level x-ray-photoemission spectra taken at ~300 and ~20 K. At 300 K, the peaks are located at 161.2, 225.6, and 780.3 eV, respectively.

of the present measurements. Contrary to this behavior, the V core-level peaks are shifted toward lower binding energies by 0–0.05 eV in going from ~300 to ~20 K, as shown in Fig. 5. The interpretation of the core-level shifts is not straightforward, but a possible cause for the observed shifts is charge transfer from S to V with decreasing temperature, i.e., an increase in the V-S covalency, possibly associated with the lattice distortion or the volume contraction. We note that the V core-level binding energies in $BaVS_3$ are close to those in V_2O_3 (V^{3+}) rather than those in the VO_2 (V^{4+}), indicating a strong covalency between the V 3*d* and S 3*p* orbitals.

In addition to the binding-energy shifts, the V 3*s* and 3*p* spectra show detectable changes in their spectral line shapes with temperature. This suggests that the V 3*d* electrons change their character with temperature, as we shall see below. In particular, the V 3*s* spectrum is narrowed in going from ~300 to ~20 K. The narrowing cannot be due to the suppression of the V^{5+}-V^{4+}-V^{3+} valence fluctuation, which exists in the metallic phase but not in the semiconducting phase with the stable valence of V^{4+}, because the same narrowing is not observed in the other V core levels. The narrowing would be due to a change in the exchange interaction between the 3*s* core hole and the incomplete 3*d* shell, because such interaction is known to be most pronounced for the 3*s* core level. Within the ionic model, the exchange splitting of the 3*s* core level is given by

$$\Delta E_{\mathrm{ex}} = \left[\frac{(2S+1)}{5}\right] G^2(2s,3d) \tag{3}$$

and the intensity ratio of the two peaks by $S/(S+1)$, where S is the total spin of the V ion and $G^2(3s,3d)$ is a Slater integral.[30] Unfortunately, both the splitting and the intensity ratio are small for the V^{4+} (d^1) ion, and cannot reliably be determined by a standard least-squares analysis of the spectral line shape. Nevertheless, the decrease in ΔE_{ex} suggests that S or $G^2(3s,3d)$ decreases at low temperatures. A decrease in S is consistent with the decrease in the effective moment as mentioned above, whereas a decrease in $G^2(3s,3d)$ could also occur as a result of the increased V-S covalency.

C. Valence-band spectra

Figure 6 shows the valence-band spectra of $BaVS_3$ taken with x-ray and ultraviolet radiation. The broad S 3*p* band extends from 1 to 8 eV below the Fermi level (E_F), and the occupied part of the V 3*d* (t_{2g}) conduction band

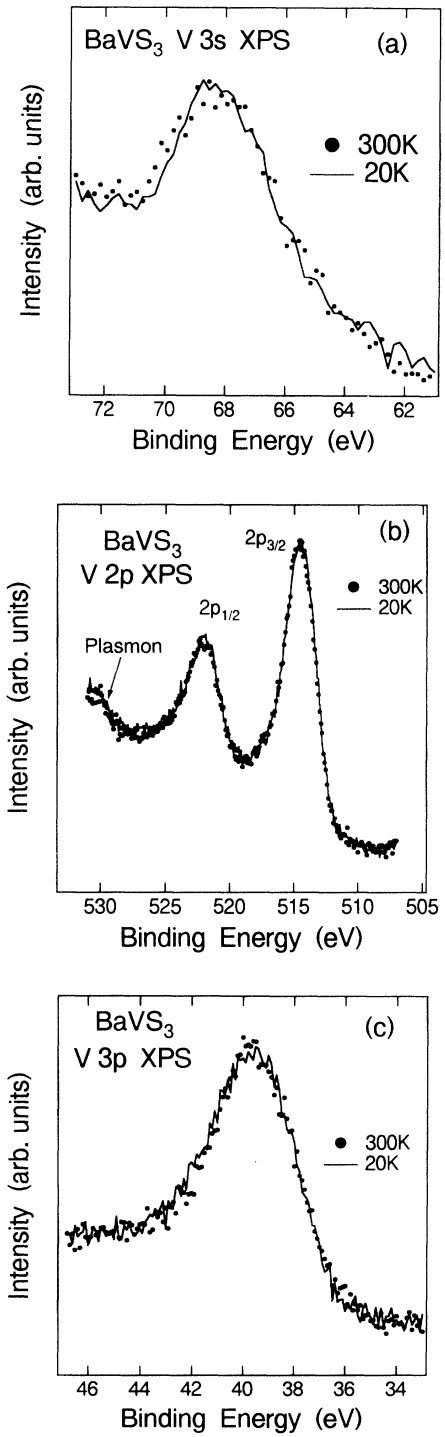

FIG. 5. V 3*s* (a), V 2*p* (b), and V 3*p* (c) core-level x-ray-photoemission spectra taken at ~300 and ~20 K.

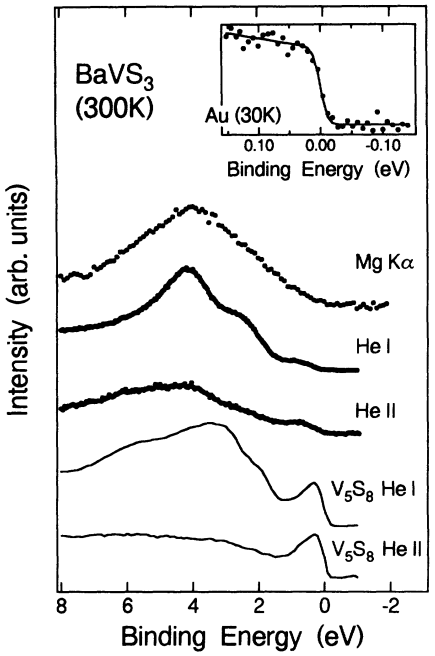

FIG. 6. Valence-band-photoemission spectra taken with Mg $K\alpha$ ($h\nu$=1253.6 eV), He I ($h\nu$=21.2 eV), and He II ($h\nu$=40.8 eV) radiation at ~300 K, compared with those of V_5S_8 (Ref. 31). The inset shows the spectrum of an evaporated Au film near the Fermi level taken with ~22-meV resolution (dots), and its least-squares analysis (solid curve) as described in the text.

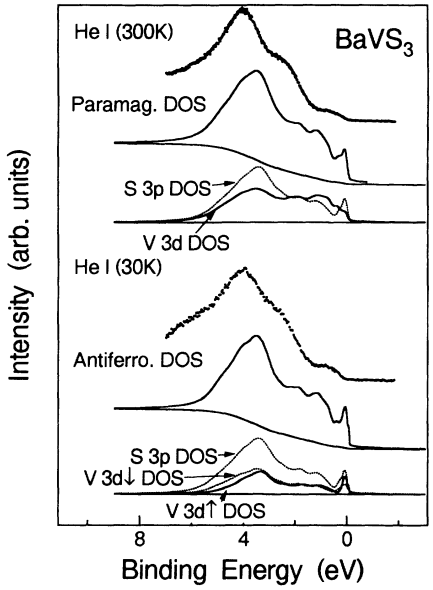

FIG. 7. Valence-band spectra taken at ~300 and ~30 K compared with the band-structure calculation (Ref. 28). The calculated DOS has been broadened using Gaussian (FMHW=22 meV) and Lorentzian [FMHW=0.4($E-E_F$)] functions, and is superimposed on the integral background.

is located within ~1.5 eV of E_F. One can see that the photoemission intensity at E_F is strikingly suppressed, and no Fermi cutoff is detected. This is contrasted with the spectra of metallic V_5S_8, having a three-dimensional metal-deficient NiAs-type structure, shown in the same figure (taken with a lower resolution of ~200 meV).[31]

A band-structure calculation has been made for $BaVS_3$ by Itoh, Fujiwara, and Tanaka.[28] We have simulated the He I valence-band spectra using the appropriately broadened density of states (DOS) of the paramagnetic state and that of the antiferromagnetic state as shown in Fig. 7. Here, the partial DOS has been multiplied by corresponding cross sections.[32] The calculated spectra both show a clear Fermi cutoff with high intensity, suggesting that the suppression of the Fermi edge is due to those effects which are not included in the band-structure calculation such as electron correlation. Thus we attribute the suppression of the Fermi-edge intensity to that characteristic of a Luttinger liquid, as proposed by recent photoemission studies on one-dimensional metals.[12-14] Apart from that discrepancy, the observed valence-band spectra correspond well to the calculated DOS: The observed peaks at ~2.5 and ~4 eV correspond to the structures located at ~2 and 3 eV in the calculated DOS. The intensity of the S 3p emission is strongly suppressed for He II because of a Cooper minimum in the photoionization cross section of the S 3p atomic orbital around this photon energy.[32] Comparison of the V 3d partial DOS with the He II spectrum leads to the same conclusion, namely the anomalous suppression of the photoemission intensity at E_F and the overall shift of the other spectral features by ~1 eV toward higher binding energies.

Figure 8 shows the temperature dependence of the valence-band spectra. In going from 300 to 130 K, the intensity of the feature at ~1 eV gradually decreases, and the intensity of the feature at ~4 eV increases. Concomitantly the peaks at ~1, ~2.5, and ~4 eV are slightly shifted toward higher binding energies. In going further down to 30 K, the intensity at ~1 eV recovers and the intensity at ~4 eV decreases again, and the peaks are shifted back toward E_F. These changes occur gradually as a function of temperature, and no abrupt changes could be observed across the crystallographic phase transition at ~240 K nor across the metal-semiconductor

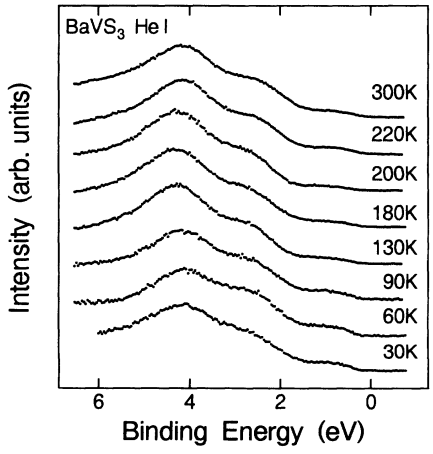

FIG. 8. Valence-band UPS spectra at various temperatures. The spectra have been normalized to the integrand photoemission intensity in the valence-band region.

transition at ~70 K. This indicates that the metal-semiconductor transition does not suddenly occur at ~70 K but that changes in the electronic structure related to the transition take place already above ~70 K. The absence of abrupt changes at ~240 K is not unexpected because the transition is of the second order, and the orthorhombic distortion gradually increases from ~240 to ~100 K (see Fig. 10). Here we note that, according to Sayetat *et al.*[19] and Ghedira *et al.*,[20] there is a dynamical distortion of the V linear chains into zigzag ones above the ~240-K transition because the thermal ellipsoids of the V atoms in the hexagonal phase are strongly anisotropic.

Figure 9 shows the temperature dependence of the He I UPS spectra in the region near E_F. Above ~220 K, a finite intensity is observed at E_F, although no clear Fermi cutoff is observed. The intensity at E_F decreases with decreasing temperature and almost disappears at ~90 K, well above the metal-to-semiconductor transition temperature ~70 K. The disappearance of the intensity at E_F is accompanied by the recovery of the ~1-eV feature (Fig. 8), which will be somehow related to the localization of the V 3*d* electrons in the semiconducting phase. These changes in the photoemission spectra near ~90 K may also be related to the fact that the magnetic susceptibility shows suppression below ~90 K compared to the Curie-Weiss law [see Fig. 3(b)].

IV. DISCUSSION

A. Origin of the metal-to-semiconductor transition at ~70 K

The origin of the metal-to-semiconductor transition at ~70 K has been controversial, and no consensus has been reached so far. The peak in the magnetic susceptibility close to this temperature lead to the suggestion that the transition is associated with an antiferromagnetic ordering. However, there has been no evidence so far of a long-range magnetic order at 35–70 K. According to the neutron-diffraction experiment, the ordered moment, if existed, should be less than $0.5\mu_B$/V.[23] The NMR experiment excluded a magnetic ordering above ~35 K.[24] Nishihara and Takano,[24] from the Knight shift, line width, and relaxation time of the ^{51}V NMR data proposed that the metal-semiconductor transition at ~70 K is accompanied by a gradual pairing of the magnetic V ions to form a nonmagnetic state with decreasing temperature. However, such a pairing has not been detected by detailed x-ray-diffraction studies,[19,20] indicating that the lattice distortion, if it exists, should be very small in contrast to the case of VO_2.[33]

Massenet *et al.*[25] have suggested that the ~70-K transition is due to the onset of a gradual electron transfer from the localized magnetic states (mainly $d_{x^2-y^2}$ and d_{xy} orbitals) to nonmagnetic states (d_z^2 orbitals) based on their Ti-substitution study. However, this model contradicts the observation that the *c*-axis parameter decreases only smoothly and slightly (by ~0.01 Å from room temperature to the lowest temperature studied), whereas the *a*- and *b*-axis parameters exhibit anomalous changes at ~70 K,[19] as shown in Fig. 10. Further, the model seems to be unable to explain the metal-to-semiconductor transition at ~70 K, since the d_z^2 orbitals, which are directed along the *c* axis, should form a wider band than the $d_{x^2-y^2}$ and d_{xy} orbitals. It therefore seems natural to consider that the temperature-dependent orthorhombic distortion below ~240 K is associated with a charge redistribution between the $d_{x^2-y^2}$ and d_{xy} orbitals, and that the occupation of the d_z^2 orbital remain almost unchanged in the whole temperature range.

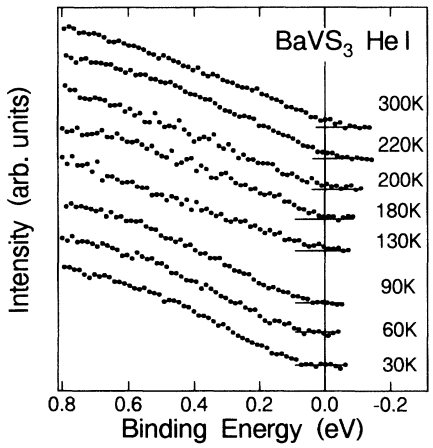

FIG. 9. Valence-band UPS spectra near the Fermi level at various temperatures. The same as in Fig. 8.

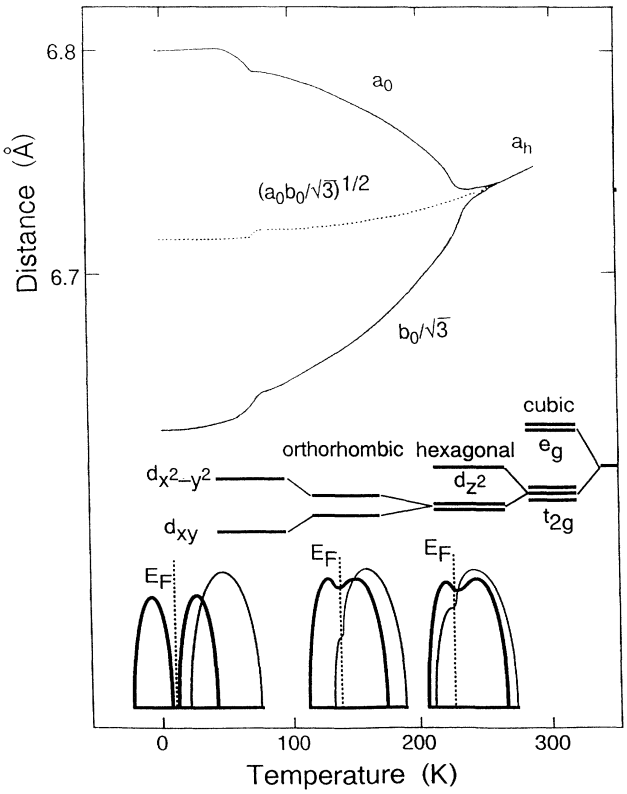

FIG. 10. Upper panel: Orthorhombic lattice parameters a_0 and b_0, of $BaVS_3$ as functions of temperature (Ref. 19). Lower panel: schematic pictures of the electronic state at various stages of the successive phase transitions.

In the octahedral coordination, the V $3d$ level is split into e_g (d_{zx} and d_{zy}) and t_{2_g} (d_z^2, d_{xy}, and $d_{x^2-y^2}$) sublevels as shown in Fig. 10. The orbitals in the t_{2g} sublevel are further split into a lower doublet (d_{xy} and $d_{x^2-y^2}$) and a higher singlet (d_z^2) due to the elongation of the VS_6 octahedra along the c axis. Along the V chain, neighboring d_z^2 orbitals directly overlap with each other and form a wide conduction band, whereas neighboring d_{xy} and $d_{x^2-y^2}$ orbitals indirectly overlap along the same direction via hybridization through the intervening S $3p$ orbitals.[22,29] The d_{xy}-$d_{x^2-y^2}$ doublet is further split by the orthorhombic distortion, as represented by the difference in the lattice parameters, $a_0-b_0/\sqrt{3}$ (Fig. 10). (Here a_0 and b_0 are the orthorhombic a- and b-axis parameters, and are related to the hexagonal lattice parameters a_h and b_h through $a_0\sim a_h$ and $b_0/\sqrt{3}\sim b_h$.) As a result, the d_{xy} orbital becomes the lowest d level. The distortion can be regarded as a cooperative Jahn-Teller distortion. Above $\sim$240 K, the orthorhombic distortion is dynamical[19,20] and therefore the d_{xy} and $d_{x^2-y^2}$ orbitals are equally populated. Below $\sim$240 K, the static distortion gradually increases with decreasing temperature down to $\sim$70 K, causing the preferential population of the d_{xy} orbitals. At $\sim$70 K, the distortion shows a discontinuous increase and then almost saturates, which we attribute to the complete transfer of electrons to the d_{xy} orbitals by electrons. At this stage, the d_{xy} band is half-filled, and a Mott-Hubbard gap opens at E_F. In going from above $\sim$70 K to below it, the intrachain V-V distance increases by $\sim$0.007 Å,[18] consistent with the Mott transition. Due to the large fluctuation effect in one dimension, the local moments of the V ions show no long-range order down to $\sim$35 K.

The above picture is consistent with the gradual change of the UPS spectra with temperature: A schematic density of states at each stage of the successive phase transitions is depicted in the lower panel of Fig. 10. The dynamical distortion above $\sim$240 K and the incomplete distortion at 70–240 K leads to the formation of a pseudogap in the d_{xy}-$d_{x^2-y^2}$ subband. This picture is further modified by electron correlation in one dimension, through which the spectral intensity at E_F is further suppressed. The apparent opening of the band gap well above $\sim$70 K may reflect a large fluctuation effect: The high electrical conductivity in this temperature range (70–90 K) in spite of the opening of the gap in the photoemission spectra may indicate that the charge transport is realized by collective excitations or by the motion of dynamical "metallic domains" on the semiconducting background. The slight suppression of the magnetic susceptibility below $\sim$90 K compared to the ideal Curie-Weiss law [Fig. 3(b)] may reflect such an "incompletely metallic" state.

As for the nature of the $\sim$35-K transition, Nishihara and Takano[24] have concluded from their NMR results that the pairing of 81% V atoms takes place below $\sim$35 K, and that 19% V atoms remain paramagnetic. This suggests that the antiferromagnetic ordering is not long-ranged but is a static, short-range one. The Curie-Weiss contribution in this temperature range of the present samples is significantly larger than those found in previous studies.[17,22,25] The fact that the Curie-Weiss contribution varies between the different studies[17,2,25] suggests that the Curie-Weiss contribution arises from unpaired spins in the disordered antiferromagnetic state. The negative Weiss constant at $T<35$ K indicates that the interaction between the paramagnetic spins are antiferromagnetic. This can be understood if we admit that the single d_{xy} orbital is occupied by one electron in this temperature range, since in this case the V-V superexchange interaction would be antiferromagnetic. The suppression of the magnetic susceptibility below $\sim$70 K is then a direct consequence of the growth of the antiferromagnetic spin correlation. The positive Weiss constant above $\sim$70 K, on the other hand, is attributed to ferromagnetic coupling between the V atoms arising from the near degeneracy of the d_{xy} and $d_{x^2-y^2}$ orbitals.[34]

The origin of the change in the paramagnetic effective moment at $\sim$160 K remains unclear in the above model. It may be related to the change in the slope of the Seebeck coefficient at $\sim$140 K identified in our data as well as in Ref. 29. Further studies are required to clarify the nature of the $\sim$160-K anomaly.

B. Luttinger-liquid behavior

As stated in Sec. III, we attribute the suppression of the photoemission intensity at E_F to the formation of a Luttinger liquid in $BaVS_3$. Therefore, we fitted the UPS spectra near E_F (within 0.3 eV of E_F) to the single-particle spectral function of a Luttinger liquid, i.e., to a power law of the electron binding energy[11] with appropriate thermal broadening [full width at half maximum (FWHM)$\sim 3.8k_BT$, following that of the Fermi-Dirac distribution] as shown in Fig. 11. (In fact, no explicit calculations exist for the spectral function of a Luttinger liquid at finite temperatures, but we consider that the above broadening procedure is a good approximation.) Since at low temperatures (<90 K) the photoemission intensity is almost completely suppressed in a finite energy

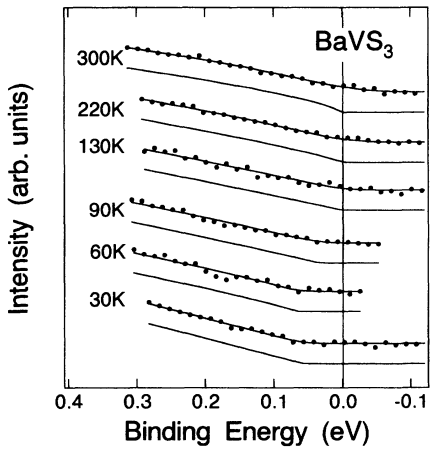

FIG. 11. Valence-band UPS spectra (dots) fitted to the power law, E^θ or $(E-E_0)^\theta$, with the instrumental and thermal broadening taken into account. Under each spectrum is shown the unbroadened power-law curve. The spectra have been normalized to the intensity at $\sim$0.3 eV.

range around E_F, we allowed a finite threshold energy $E_0(>0)$ to vary with temperature together with the power-law exponent θ. Thus our model spectral function at $T=0$ has the form[11]

$$\rho(E) \propto [E - E_0(T)]^{\Theta(T)} , \tag{4}$$

where E is the electron binding energy measured from E_F. (When $E_0 > 0$, the system is not metallic, so that the exponent θ loses its original physical meaning.) Since the power-law behavior of the spectral function is strictly valid only in the vicinity of E_F, the θ and E_0 values thus obtained (Fig. 12) may depend on the fitted energy range. In order to test this possibility, we varied the upper bound for the binding energy used for the fitting between 0.3 and 0.1 eV, and found that the θ and E_0 did not change to within ± 0.05 and ± 5 meV, respectively. For an even smaller energy range, the fitting iteration became unstable, particularly for the high-temperature data, where thermal broadening is comparable to the fitted energy range. Therefore, we consider that the θ and E_0 obtained above well represent the low-energy behavior of the spectral function.

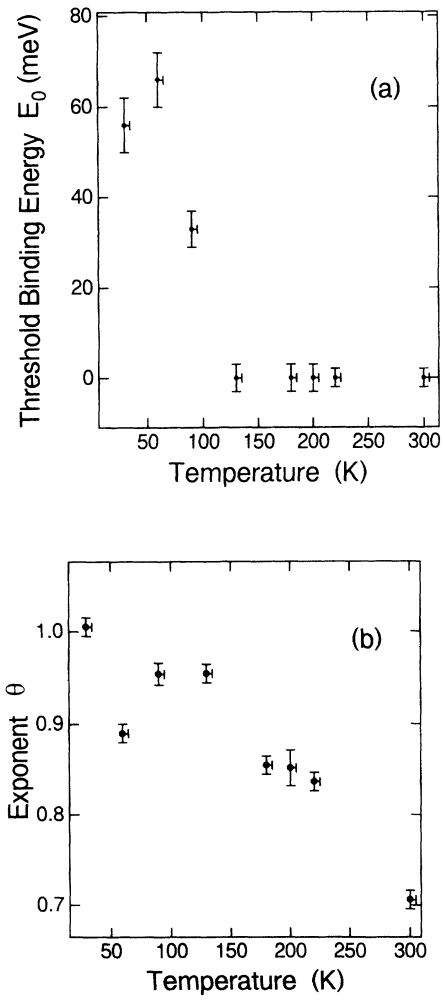

FIG. 12. Temperature dependence of the threshold binding energy E_0 (a) and the exponent θ (b).

As shown in Fig. 12(a), the threshold binding energy is found to be zero from 300 to 130 K, and increases below ~ 100 K at ~ 65 meV. The finite E_0 at 90 K, well above the metal-to-semiconductor transition temperature, is surprising. We cannot completely exclude the possibility that the finite E_0 is an artifact of the fitting procedure using Eq. (4). Nevertheless, it can be safely concluded that the intensity at E_F is unusually suppressed already well above the transition temperature ~ 70 K. Indeed, one notices a slight increase in the electrical resistivity below ~ 120 K (Fig. 2; see also Ref. 17), which may be an indication of the depletion of the electronic states at E_F or the opening of a (pseudo)gap well above ~ 70 K.

In the metallic state above ~ 130 K, we can conclude from the success of the power-law fit of the spectra that the metallic electrons in $BaVS_3$ form a Luttinger liquid, at least on the energy scale of $\sim k_B T$. (The spectrum taken at 300 K could also be fitted with a small but finite Fermi edge. However, strict distinction between a Fermi liquid with a small spectral intensity at E_F and a Luttinger liquid with strictly vanishing intensity at E_F is not meaningful under the influence of the strong thermal broadening effect at ~ 300 K.) Figure 12(b) shows that the exponent θ increases from ~ 0.71 at 300 K, to ~ 0.85 at 130 K. Theoretically, for the one-dimensional Hubbard model with on-site Coulomb repulsion U, θ cannot exceed $\frac{1}{8}$ for a single-band [$SU(2)$] model,[8] and $\frac{9}{32}$ for a degenerate two-band [$SU(4)$] model.[35] For a model with long-range interaction (e.g., with $1/r^2$ interaction), on the other hand, θ can be arbitrarily large for strong interaction.[7] Therefore, the observed large θ values indicate that the Hubbard model is not sufficient to treat electron correlation in the present system, and that the electron-electron interaction is probably long ranged. For $(TMTSF)_2PF_6$, θ is found to be larger ~ 2,[12] indicating that the interaction is more long-ranged in the organic conductor than in $BaVS_3$.

In the following, we will make use of the universal scaling for Luttinger liquids to discuss the physical properties of $BaVS_3$. For an $SU(2)$ model, the charge-density correlation function can be written as

$$\langle n(r)n(0)\rangle \sim \text{const} + A_0 r^{-2} + A_2 r^{-\beta_{2k_F}} \cos(2k_F r) + A_4 r^{-\beta_{4k_F}} \cos(4k_F r) , \tag{5}$$

(neglecting logarithmic corrections),[8] where $n(r)$ is the density operator at the lattice site r, k_F is the Fermi wave number, and A_0, A_2, and A_4 are constants. For an $SU(4)$ model, $6k_F$ and $8k_F$ terms are added to Eq. (5). For the spin-correlation function $\langle s_z(r)s_z(0)\rangle$, the $4k_F$ term does not appear for the $SU(2)$ model, nor the $8k_F$ term for the $SU(4)$ model. For a small correlation exponent β_i, the corresponding correlation length becomes large. Therefore, the instability of the Luttinger liquid toward spin-density-wave (SDW) or charge-density-wave (CDW) formation (e.g., under the influence of finite interchain interaction) is represented by the smallness of the corresponding critical exponent β_i. For an $SU(2)$ model, the $2k_F$ SDW instability corresponds to antiferromagnet-

ic ordering with two electrons in a wavelength, and the $2k_F$ CDW instability corresponds to the pairing of two electrons in a charge-density peak. The $4k_F$ CDW instability corresponds to the formation of a Wigner crystal, which is equivalent to a transition to a Mott insulator for one electron per atomic site. For an $SU(4)$ model, k_F becomes half of the k_F of the $SU(2)$ model with the same electron density. Then Wigner crystallization (and hence the Mott transition) results from the instability of the $8k_F$ CDW and the electron pairing is given by the $4k_F$ CDW. θ is related to β_{4k_F} or β_{8k_F} through[8]

$$\theta=(\beta_{4k_F}-4)^2/16\beta_{4k_F}, \tag{6}$$

for the $SU(2)$ model, and through

$$\theta=(\beta_{4k_F}-4)^2/16(\beta_{4k_F}-2), \tag{6'}$$

$$\theta=(\beta_{8k_F}-8)^2/64\beta_{8k_F} \tag{6''}$$

for the $SU(4)$ model.[36] For both models, β_{2k_F}, β_{4k_F}, and β_{8k_F} are related through

$$\beta_{2k_F}=1+\beta_{4k_F}/4\ , \tag{7}$$

$$\beta_{4k_F}=2+\beta_{8k_F}/4\ . \tag{7'}$$

These relations are plotted in Fig. 13.

In order to consider the instability of the Luttinger liquid in $BaVS_3$ toward the semiconducting state below $\sim$70 K, let us consider a hypothetical metallic state of $BaVS_3$ where the d_{xy} band is occupied by nearly one ($\lesssim 1$) electron per V atom [$SU(2)$ model], and discuss its instability toward the $2k_F$ and $4k_F$ modulations mentioned above. For $\theta=0.8$–0.9 deduced from the photoemission spectra, we find from Fig. 13 that β_{4k_F} ($\sim$0.9) is smaller than β_{2k_F} ($\sim$1.2), meaning that the $4k_F$ instability dominates over the $2k_F$ instabilities. This explains the appearance of the Mott-insulating state without magnetic ordering nor Peierls-type CDW just below $\sim$70 K.

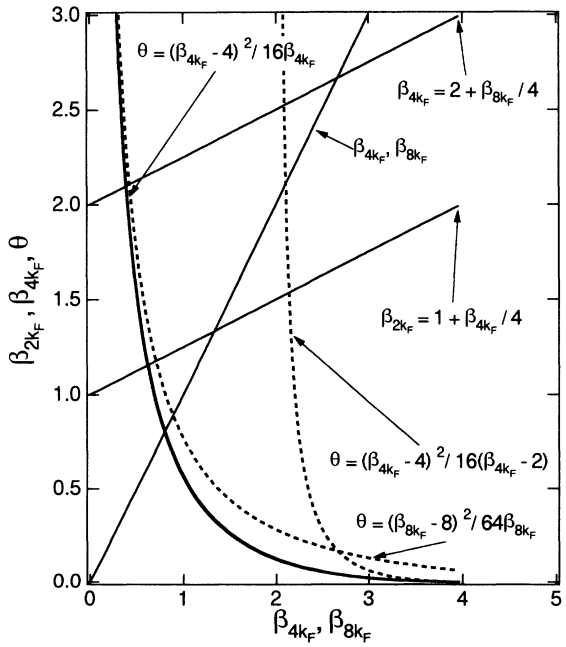

FIG. 13. Relations between the exponents θ, β_{2k_F}, β_{4k_F}, and β_{8k_F}. θ is plotted as a function of β_{4k_F} or β_{8k_F}, by solid and dashed lines, respectively, for the single-band [$SU(2)$] and degenerate two-band [$SU(4)$] models.

At high temperatures, the orthorhombic distortion is small, and thus the orbital degeneracy can effectively become close to 2 as a result of the coalescence of the d_{xy} and $d_{x^2-y^2}$ subbands. Then one can see from Fig. 13 that all the correlation exponents become large ($\beta_{2k_F}\sim 1.3$, $\beta_{4k_F}\sim 1.1$, and $\beta_{8k_F}\sim 2.3$), leading to the suppression of long-ranged spin and charge correlation at high temperatures, again consistent with the experimental observation. Even if there were no coalescence of the d_{xy} and $d_{x^2-y^2}$ subbands, the decrease in θ by $\sim$0.2 in going from $T\sim 300$ K to $T\sim 30$ K indicates some increase in β_{2k_F} and β_{4k_F}.

The temperature dependence of θ and E_0 plotted in Fig. 12 is worth further remarks. E_0 starts to increase around 100 K, increases toward $\sim$70 K, and then saturates. On the contrary, θ gradually increases with decreasing temperature from $\sim$300 to $\sim$100 K. The increase in θ cannot be due to an increase in the electron-electron interaction strength such as U, since it should be temperature independent. The gradual increase in θ can most naturally be associated with the change in the d_{xy}-$d_{x^2-y^2}$ splitting, and hence with the change in the effective orbital degeneracy. Unfortunately, there has been no theoretical studies of the orbital degeneracy dependence of the exponent θ with the other conditions fixed.

Throughout the present analyses, we have not explicitly considered the possible effect of electron-phonon interaction on the Luttinger-liquid behavior of the V $3d$ electrons. Although the interaction does not lead to a Peierls-type instability in $BaVS_3$, it may modify the dynamical properties of the Luttinger liquid and hence the correlation exponents. Even under the influence of electron-phonon interaction, we expect that the scaling relations (6) and (7) remains valid as they were universal relations independent of the form of electron-electron interaction. Then the electron-phonon interaction might be a cause for the large θ other than the long-range electron-electron interaction. In any case, the standard Hubbard model with only on-site Coulomb repulsion is not sufficient to study electron correlation effects in $BaVS_3$. This conclusion would not be restricted to one-dimensional $BaVS_3$, but would be applicable to a wider range of transition-metal chalcogenides including three-dimensional compounds. The same is true for transition-metal oxides, because the observed θ appears to be much larger than the upper limit for the Hubbard models.[17] These facts imply that reinvestigation of the physical properties of transition-metal compounds is necessary using theoretical models with long-range Coulomb interaction and possibly with electron-phonon interaction.

C. Semiconducting state

In a semiconductor, the threshold energy E_0 deduced from photoemission spectra would be equal to the activation energy of the p-type electrical conductivity. Indeed, the electrical conductivity of $BaVS_3$ is of the p type in the semiconducting phase,[29] and the activation energy of the present sample deduced from the electrical resistivity is ~ 25 meV between ~ 40 and ~ 80 K, being of the same order of magnitude as the photoemission threshold energies (~ 30 meV at ~ 90 K and ~ 62 meV at ~ 60 K). The generally larger values deduced from photoemission may be attributed to a polaronic effect.[36]

The density of states of one-dimensional insulators should show a $\sim E^{-0.5}$ divergence at the band edges irrespective of the origin of the band gap, i.e., irrespective of whether the band gap is due to the one-electron band structure or to electron correlation (Mott insulator).[7] We could not observe such a divergence in the spectra of the semiconductor phase (Fig. 9), however, either because the divergence occurs on an energy scale smaller than our instrumental resolution or because there is a finite interaction between the V chains, which leads to the suppression of the one-dimensional character. The latter interpretation is consistent with the presence of the antiferromagnetic ordering, indicative of finite interchain interaction.

V. CONCLUSION

We have studied the electronic structure of $BaVS_3$ by UPS, XPS, electrical-resistivity, and magnetic-susceptibility measurements. High-resolution UPS spectra near the Fermi level in the metallic phase exhibit a power-law dependence of the electron binding energy, indicating that the conduction electrons in $BaVS_3$ form a Luttinger liquid. The spectra exhibit gradual changes with varying temperature. In particular, a semiconducting gap starts to open well above the metal-to-semiconductor transition temperature, and develops fully below it. The exponent θ of the photoemission spectra in the vicinity of the Fermi level is large ($\lesssim 1$), which means that the electron-electron interaction is rather long ranged (and possibly that electron-phonon interaction is also important). As for the origin of the ~ 70-K phase transition, we propose that the orthorhombic distortion, which gradually increases below ~ 240 K with decreasing temperature, lowers one of the d levels, d_{xy}. The d_{xy} band becomes half-filled below ~ 70 K, when electrons are fully transferred to the latter band, resulting in the opening of a Mott-Hubbard gap. In the Mott-insulating state, antiferromagnetic coupling exits between the V spins but does not lead to a static magnetic order above ~ 35 K, and below this temperature a static short-range order develops. The large θ implies the instability of the Luttinger liquid toward a Mott insulator for the single-band (d_{xy} band) model, consistent with the appearance of the semiconducting state without magnetic ordering just below ~ 70 K.

ACKNOWLEDGMENTS

We thank Professor Y. Takakuwa for advice in designing and manufacturing the He discharge lamp, Dr. Y. Murakami for kindly performing the SQUID measurements, and A. Tsujinouchi for his assistance in the preparation of the sample. We have greatly benefited from discussions with Professor N. Kawakami on the theoretical aspects of one-dimensional electron systems. We also thank Professor H. Nishihara for discussion of the NMR results and Dr. T. Itoh and Professor T. Fujiwara for use of the result of the band-structure calculation on $BaVS_3$ prior to publication. This work was supported by a Grant-in-Aid from the Ministry of Education, Science and Culture, Japan, and the Toray Science Foundation.

*Also at Department of Physics, Science University of Tokyo, Tokyo, Japan.

†Present address: Department of Materials Science, Hiroshima University, Higashi-Hiroshima, Hiroshima 724, Japan.

[1]R. E. Peierls, in *Quantum Theory of Solids* (Oxford, Clarendon, 1964).

[2]J. M. Luttinger, J. Math. Phys. **4**, 1154 (1963).

[3]S. Tomonaga, Prog. Theor. Phys. **5**, 349 (1950).

[4]F. D. M. Haldane, Phys. Rev. Lett. **45**, 1358 (1980).

[5]J. Sólyom, Adv. Phys. **28**, 210 (1979).

[6]M. Ogata and H. Shiba, Phys. Rev. B **41**, 2326 (1990).

[7]N. Kawakami and S.-K. Yang, Phys. Rev. Lett. **67**, 2493 (1991).

[8]N. Kawakami and S.-K. Yang, Phys. Lett. A **148**, 359 (1990).

[9]N. Kawakami and A. Okiji, Phys. Rev. B **40**, 7066 (1989).

[10]H. J. Schulz, Phys. Rev. Lett. **64**, 2831 (1990).

[11]V. Meden and K. Schönhammer, Phys. Rev. B **46**, 15 753 (1993); K. Schönhammer and V. Meden, J. Electron Spectrosc. Relat. Phenom. **62**, 225 (1993); J. Voit, J. Phys. Condens. Matter **5**, 8305 (1993).

[12]B. Dardel, D. Malterre, M. Grioni, P. Weibel, Y. Baer, and F. Lévy, Phys. Rev. Lett. **67**, 3144 (1991).

[13]B. Dardel, M. Grioni, D. Malterre, P. Weibel, Y. Baer, J. Voit, and D. Jérôme, Europhys. Lett. **24**, 687 (1993).

[14]Y. Hwu, P. Alméras, M. Marsi, H. Berger, F. Lévy, M. Grioni, D. Malterre, and G. Margaritondo, Phys. Rev. B **46**, 13 624 (1992).

[15]R. A. Gardner, M. Vlasse, and A. Wold, Acta Crystallogr. Sec. B **25**, 781 (1969).

[16]G. N. Tishchenko, Trans. Inst. Kristtallogr. Akad. Nauk SSSR **11**, 93 (1955).

[17]M. Takano, H. Kosugi, N. Nakanishi, M. Shimada, T. Wada, and M. Koizumi, J. Phys. Soc. Jpn. **43**, 1101 (1977).

[18]M. Ghedira, J. Chenavas, F. Savetat, and M. Marezio, Acta Crystallogr. Sec. B **37**, 1491 (1981).

[19]F. Sayetat, M. Ghedira, J. Chennavas, and M. Marezio, J. Phys. C **15**, 1627 (1982).

[20]M. Ghedira, M. Anne, J. Chennavas, M. Marezio, and F. Sayetat, J. Phys. C **19**, 6489 (1986).

[21]M. Shimada, M. Koizumi, M. Takano, N. Nakanishi, and E. K. Graham, Jpn. J. Appl. Phys. **18**, 717 (1979).

[22]O. Massenet, R. Buder, J. J. Since, C. Schlenker, J. Mercier, J. Kelber, and D. G. Stucky, Mater. Res. Bull. **13**, 187 (1978).

[23]J. Kelber, A. T. Aldred, G. H. Lander, M. H. Mueller, O.

Massenet, and G. D. Stucky, J. Solid State Chem. **32**, 351 (1980).
[24]H. Nishihara and M. Takano, J. Phys. Soc. Jpn. **50**, 426 (1981).
[25]O. Massenet, J. J. Since, J. Mercier, M. Avignon, R. Buder, and V. D. Nguyen, J. Phys. Chem. Solids **40**, 573 (1979).
[26]A. Heideman and M. Tanako, Phys. Status Solidi **100**, 343 (1980).
[27]R. Itti, T. Wada, K. Matuura, T. Itoh, K. Ikeda, H. Yamauchi, N. Koshizuka, and S. Tanaka, Phys. Rev. B **44**, 2306 (1991).
[28]T. Itoh, T. Fujiwara, and S. Tanaka (unpublished).
[29]K. Matsuura, T. Wada, T. Nakamizo, H. Yamauchi, and S. Tanaka, Phys. Rev. B **43**, 13 118 (1991).
[30]D. A. Shirley, in *Photoemission in Solids I*, edited by M. Cardona and L. Ley (Springer-Verlag, Berlin, 1978), p. 167.
[31]A. Fujimori, M. Saeki, and H. Nozaki, Phys. Rev. B **44**, 163 (1991).
[32]J. J. Yeh and I. Lindau, At. Data Nucl. Data Tables **32**, 1 (1985).
[33]A. Zylbersztejn and N. F. Mott, Phys. Rev. B **11**, 4983 (1975).
[34]M. Cyrot and C. Lyon-Caen, J. Phys. (Paris) **36**, 253 (1975).
[35]N. Kawakami, Phys. Rev. B **46**, 3191 (1992); **47**, 2928 (1993).
[36]H. Namatame, A. Fujimori, H. Takagi, S. Uchida, F. M. F. de Groot, and J. C. Fuggle, Phys. Rev. B **48**, 16 917 (1993).